

UC San Diego

UC San Diego Previously Published Works

Title

Activity of the HMGB1-derived immunostimulatory peptide Hp91 resides in the helical C-terminal portion and is enhanced by dimerization

Permalink

<https://escholarship.org/uc/item/4kz181hz>

Journal

Molecular Immunology, 57(2)

ISSN

0161-5890

Authors

Saenz, R
Messmer, B
Futalan, D
[et al.](#)

Publication Date

2014-02-01

DOI

10.1016/j.molimm.2013.09.007

Peer reviewed



Published in final edited form as:

Mol Immunol. 2014 February ; 57(2): 191–199. doi:10.1016/j.molimm.2013.09.007.

Activity of the HMGB1-Derived Immunostimulatory Peptide Hp91 Resides in the Helical C-terminal Portion and is Enhanced by Dimerization

R. Saenz^a, B. Messmer^a, D. Futalan^a, Y. Tor^b, M. Larsson^c, G. Daniels^a, S. Esener^{a,d}, and D. Messmer^a

^aRebecca and John Moores Cancer Center, University of California San Diego (UCSD), La Jolla, CA 92093, USA

^bDepartment of Chemistry and Biochemistry, UCSD

^cDepartment of Clinical and Experimental Medicine, Linköping University, Sweden

^dDepartment of NanoEngineering, UCSD, La Jolla, CA

Abstract

We have previously shown that an 18 amino acid long peptide, named Hp91, whose sequence corresponds to a region within the endogenous protein HMGB1, activates dendritic cells (DCs) and acts as adjuvant *in vivo* by potentiating Th1-type antigen-specific immune responses. We analyzed the structure-function relationship of the Hp91 peptide to investigate the amino acids and structure responsible for immune responses. We found that the cysteine at position 16 of Hp91 enabled formation of reversible peptide dimers, monomer and dimer were compared for DC binding and activation. Stable monomers and dimers were generated using a maleimide conjugation reaction. The dimer showed enhanced ability to bind to and activate DCs. Furthermore, the C-terminal 9 amino acids of Hp91, named UC1018 were sufficient for DC binding and Circular dichroism showed that UC1018 assumes an alpha-helical structure. The ninemer peptide UC1018 induced more potent antigen-specific CTL responses *in vivo* compared to Hp91 and it protected mice from tumor development when used in a prophylactic vaccine setting. We have identified a short alpha helical peptide that acts as potent adjuvant inducing protective immune responses *in vivo*.

Introduction

Immune adjuvants that enhance the quality and longevity of an immune response are important components of subunit vaccines. Aluminum salts (alum) have been used as vaccine adjuvants for over a century. However, alum induces primarily humoral, Th2-type

Corresponding author: Bradley Messmer Ph.D., Moores Cancer Center, University of California San Diego, 3855 Health Sciences Dr., Room 5312, La Jolla, CA, 92093-0815, Tel.858-534-1783, FAX.858-822-6333, bmessmer@ucsd.edu.

Publisher's Disclaimer: This is a PDF file of an unedited manuscript that has been accepted for publication. As a service to our customers we are providing this early version of the manuscript. The manuscript will undergo copyediting, typesetting, and review of the resulting proof before it is published in its final citable form. Please note that during the production process errors may be discovered which could affect the content, and all legal disclaimers that apply to the journal pertain.

immune responses, which are undesirable for vaccination against certain viruses, intracellular pathogens, and cancer (1). Development of new, safe adjuvants that stimulate a cellular, Th1-type immune response could expand vaccine development to permit protection and recovery from these pathogens and cancers.

Rapid advances in vaccine development have recently led to an expanding number of vaccines containing adjuvants other than aluminum salts (alum): 1) the FDA-approved HPV vaccine, Cervarix®, and the European Medicines Agency-approved HBV and seasonal allergy vaccines, Fendrix® and Pollinex Quattro® respectively, are formulated with the bacterial lipoprotein MPL as adjuvant, and 2) several influenza vaccines in Europe are formulated with squalene (e.g. MF59) as adjuvant (2). With the success of these newly approved vaccines comes an intensified search for additional immune adjuvants. We have previously shown that an 18 amino acid (aa) long peptide named Hp91, whose sequence corresponds to a portion of the HMGB1 protein, acts as a potent Th1-stimulating adjuvant *in vivo* (3). By understanding the structure-function relationship of peptide adjuvants one may gain the ability to engineer more potent versions based on active regions or important structural elements. Here, we performed structure-function relationship studies to help us understand and enhance the adjuvant activity of Hp91.

HMGB1, originally described as a nuclear binding protein that facilitates DNA bending and nucleosome formation (4), was previously shown to act as an endogenous adjuvant (5). HMGB1 is highly conserved and besides its nuclear functions, it is actively released by monocytes and macrophages following exposure to LPS, TNF α , and IL-1 β and passively released during cell injury and necrosis (6, 7). When released from a cell, HMGB1 acts as an endogenous danger signal, stimulating cytokine release from monocytes, macrophages, and dendritic cells (DCs) (6, 8). HMGB1 was shown to act as adjuvant to delay tumor growth and increase tumor-free survival in mice (5). The proinflammatory region of HMGB1 has been mapped to its B box domain, and this region is sufficient to cause DC maturation and Th1 polarization (9).

Hp91, a short peptide located within the B box domain of HMGB1, induces DC maturation and stimulates secretion of several pro-inflammatory cytokines, including the Th1 driving cytokine IL-12 (10). We recently demonstrated that Hp91 acts as adjuvant, potentiating cellular and humoral immune responses *in vivo* (3). Specifically, Hp91 promotes the *in vivo* production of immunomodulatory cytokines and activation of antigen-specific CD8⁺ T cells (3).

Hp91 contains a cysteine residue at amino acid position 16 that corresponds to Cys106 in the HMGB1 protein. This Cys106 has been shown to be critical for HMGB1 binding to TLR4 as well as inducing TNF secretion by macrophages (11). Other studies have shown that this cysteine is retained in a reduced form *in vivo* and may be responsible for nucleocytoplasmic shuttling of HMGB1 (12), and perhaps that the predominant form of serum HMGB1 can switch redox states between a reduced form during inflammation to an oxidized form during resolution of the inflammatory state (13).

Previous work investigating the structure of the HMG-box family of proteins, of which HMGB1 is a member, suggests there may be an alpha helix in the region of HMGB1 that corresponds to the C-terminal portion of Hp91 (14). In addition, the N-terminal half of the Hp91 peptide contains two PXXP motifs (Hp91 sequence: **DPNAPKRPPSAFFLFCSE**) that could break a traditional alpha helix and contribute to a left-handed polyproline II type helix (15–17). The significance of these N-terminal and C-terminal domains had not previously been considered, and their predicted secondary structures or signaling potential could contribute to the immune activity of Hp91. We show that investigating the structure-function relationships of Hp91 may allow engineering and development of potent new immunomodulatory, Th1-type adjuvant peptides.

Materials and Methods

Animals

Female C57BL/6 mice 8–12 weeks of age were used for experiments. C57BL/6 mice were purchased from Charles River Laboratories (Boston, MA). Mice were bred and maintained at the Moores UCSD Cancer Center animal facility and all animal studies were approved by the Institutional Animal Care and Use Committee of UCSD and were performed in accordance with the institutional guidelines.

Reagents

The peptides, including Hp91 (DPNAPKRPPSAFFLFCSE), UC18 (DPNAPKR), UC411 (APKRPPSA), UC714 (RPPSAFFL), UC1018 (SAFFLFCSE), and the MHC-Class I (H-2K^b)-restricted peptide epitope of ovalbumin “OVA-I” (SIINFEKL) were synthesized by GenScript Corp (Piscataway, NJ) and CPC Scientific (San Jose, CA). Peptides were routinely synthesized with greater than 95% purity. HMGB1-derived peptides were synthesized with N-terminal modifications: N-terminally biotinylated peptides were used for most experiments as previously discussed (10), except in maleimide experiments where biotin would interfere with chemical reactions and an N-terminal acetyl protecting group or fluorescent dye (CP488; CPC Scientific) was used in place of the biotin. Peptides were dissolved in RPMI for most *in vitro* experiments, and PBS for *in vivo* and HPLC experiments.

HPLC

Peptides were evaluated by HPLC (Agilent 1100 Series, Software: ChemStation, Agilent, Santa Clara, CA) at 211nm on a ZORBAX RP C18 column (Agilent). Percent dimer was calculated as the area under the curve (AUC) of dimer/(AUC of monomer + AUC of dimer) using ChemStation software (Agilent).

Maleimide conjugation reactions

Hp91 peptide monomers, capped at the thiol group of the cysteine, were generated using an N-Ethylmaleimide (NEM) (Thermo Scientific, Pittsburgh, PA) conjugation reaction. Briefly, Hp91 was dissolved in PBS and reacted for 2 h at RT in the presence of NEM. Hp91 peptide maleimide dimers, cross-linked at the thiol group of the cysteine, were generated using a Bis-maleimidoethyleneglycol (BM(PEG)₂) (Thermo Scientific) conjugation reaction.

Briefly, Hp91 was dissolved in PBS/EDTA and reacted for 1 h at RT in the presence of BM(PEG)₂. Excess NEM or BM(PEG)₂, respectively, was removed by dialysis (2K MWCO cassette, Thermo Scientific). Un-reacted, mock peptide controls were generated under identical reaction and dialysis conditions, while excluding the NEM or BM(PEG)₂ reagent. Reagents, glassware, and reaction products were endotoxin-free as determined by the manufacturer or a limulus amoebocyte assay (LAL) (Cambrex Corporation, East Rutherford, NJ) tested according to manufacturer's instructions. As the N-terminal biotin would interfere with the maleimide reactions, peptides with a Cp488 fluorescent dye at the N-terminal group were used for binding/uptake experiments. Peptides with an acetyl at the N-terminal group were used for DC stimulation experiments. For some experiments, the peptides were incubated for 30 minutes +/- 10 mM dithiothreitol (DTT) (Thermo Fischer Scientific, Pittsburgh, PA).

Generation of human immature monocyte-derived DCs (iDCs)

Peripheral blood mononuclear cells were isolated from the blood of normal volunteers over a Ficoll-Hypaque (Amersham Biosciences, Uppsala, Sweden) density gradient. Anonymous blood was purchased from the San Diego Blood Bank; therefore, no institutional review board approvals were necessary. To generate DCs, CD14⁺ progenitor cells were isolated from peripheral blood mononuclear cells using CD14 magnetic microbeads (Miltenyi Biotec, Auburn, CA) over a MACS LS column (Miltenyi Biotec), following the manufacturer's protocol. The purified CD14⁺ cells were cultured in RPMI 1640 medium (Invitrogen, Carlsbad, California) supplemented with 50mM 2-mercaptoethanol (Sigma-Aldrich, St. Louis, Missouri), 10mM HEPES (Invitrogen), penicillin (100U/ml) - streptomycin (100µg/ml) - L-glutamine (2mM) (PSG; Invitrogen), and 5% (vol/vol) human AB serum (Gemini Bio Products, West Sacramento, CA), supplemented with 1000 U/ml GM-CSF (Bayer HealthCare Pharmaceuticals, Wayne, NJ), and 200 U/ml interleukin-4 (IL-4; R and D Systems, Minneapolis, MN) at days 0, 2, and 4. Immature DCs were harvested on days 5–7.

Stimulation of iDCs

On days 5–7 of culture, iDCs were either left untreated or were stimulated with 90 µM of Hp91 or the truncated Hp91 peptides. LPS (E. coli serotype 026:B6, Sigma-Aldrich) was used as a positive control in all experiments. Supernatants were collected 48 h after stimulation and analyzed for IL-6 by ELISA (eBioscience, Inc. San Diego, CA) according to the manufacturer's instructions.

Cellular uptake studies

iDCs were pre-cooled on ice for 30 minutes. Cells were subsequently incubated with the indicated biotinylated peptides at 90µM for 30 minutes at 37°C in culture medium. Cells were washed, permeabilized with Cytofix/Cytoperm (BD Biosciences, Franklin Lakes, NJ) stained with streptavidin-Alexa 488 (Invitrogen), and analyzed by flow cytometry. Cells were immediately analyzed by flow cytometry using the FACSCalibur (Beckon Dickinson, Franklin Lakes, NJ). Data were analyzed using the FlowJo software (Tree Star, Inc., Ashland, OR).

Circular dichroism

To perform the CD experiment, we dissolved peptides in a trifluoroethanol (TFE) buffer (75%/25% TFE/H₂O by volume) (Sigma-Aldrich), which enhances polypeptide folding (18). CD spectra of peptides were collected on an AVIV model 202 Circular Dichroism Spectrometer (AVIV Biomedical, Inc., Lakewood, NJ), under nitrogen, using a 1mm pathlength quartz cuvette. These spectra were corrected by subtraction of a “solvent-only” spectrum and smoothed with GraphPad software version 5.01 for Windows (GraphPad Software, San Diego, CA). The spectra are shown in mean residue ellipticity (θ_{mrw}). Peptides were analyzed at 200 μ g/ml.

OVA Immunization

Mice were immunized s.c. with 50 μ g of OVA-I (SIINFEKL) peptide co-administered with PBS, or equimolar doses of Hp91 (250 μ g), UC714 (129 μ g), or UC1018 (142 μ g). Peptides were resuspended in PBS for all immunizations. Mice were boosted two weeks later and spleens and blood were collected one week after the final immunization. Single cell suspensions of splenocytes were prepared by mechanical disruption and separation through a 70 mm nylon cell strainer (BD Biosciences). Red blood cells were lysed using ammonium chloride buffer (Roche Diagnostics, Indianapolis, IN) and the splenocytes were subsequently resuspended in RPMI 1640 medium (Invitrogen) supplemented with 10mM HEPES (Invitrogen), penicillin (100U/ml), streptomycin (100 μ g/ml), L-glutamine (2mM) (Invitrogen), and 5% (vol/vol) fetal calf serum (Omega).

Enzyme-linked immunospot assay

Freshly isolated splenocytes were plated in duplicate to wells of an Immobilon-P (PVDF) bottom enzyme-linked immunospot (ELISpot) plate (Millipore, Billerica, MA, USA) that had been previously coated overnight with 5 μ g/ml monoclonal anti-mouse IFN- γ antibody (Mabtech, Stockholm, Sweden). Splenocytes were cultured overnight at 37°C with 2.5 μ g/ml OVA-I (SIINFEKL) peptide, 5 μ g/ml concanavalin A positive control (Sigma-Aldrich), or left unstimulated (medium only). After 18 hours, ELISpot plates were developed using 1 μ g/ml biotinylated anti-mouse IFN- γ antibody (Mabtech), Streptavidin-HRP (Mabtech), and TMB Substrate (Mabtech). The plate was scanned and the spots were counted using an automated ELISpot Reader System (CTL ImmunoSpot, Shaker Heights, OH, USA).

Cytokine Release Assay

Splenocytes were cultured overnight with 2.5 μ g/ml OVA-I (SIINFEKL) peptide, 5 μ g/ml concanavalin A positive control (Sigma-Aldrich), or left unstimulated (media only). After 18 h, cell culture supernatants were collected and analyzed for the presence of IL-2 by ELISA (eBioscience) according to manufacturer’s recommendations.

Tumor Challenge

The murine melanoma B16.F1 cell line, a gift from Richard Vile (Mayo), was cultured in Dulbecco’s modified Eagle’s Medium (DMEM) (Mediatech, Manassas, VA), supplemented with 10mM HEPES (Invitrogen), penicillin (100U/ml), streptomycin (100 μ g/ml), L-

glutamine (2mM) (Invitrogen), and 10% (vol/vol) fetal calf serum (Omega Scientific, Tarzana, CA). By injecting apoptotic B16 cells, we were able to use the entire antigenic content of the tumor cells(19). To induce apoptosis of B16 cells, the cells were treated with 0.5 mg/ml mitomycin C (Sigma-Aldrich) in DMEM media for 60 min at 37°C. Cells were washed twice in warm DMEM and put back to culture overnight in DMEM supplemented as above. Mice were immunized s.c. with 2×10^5 apoptotic mitomycin-C (Sigma-Aldrich)-treated B16 cells co-administered with either PBS or UC1018 (142µg). Mice were boosted twice, at 4 weeks and 6 weeks post-prime as above, and challenged s.c. into the flank with 2×10^5 live B16 cells at one week post-boost. Mice were followed for tumor growth and survival. Tumor dimensions were measured using calipers and the tumor volume calculated using the following formula; volume = $4/3 \pi (a^2 \times b)$. Mice were euthanized when tumor volume reached 1.5 cm³. Tumor survival curves were generated, wherein the day of euthanasia was considered as death.

Statistical analysis

Data represented are mean \pm SEM. Data were analyzed for statistical significance using unpaired or paired Student's *t*-test or the Log Rank test. Statistical analysis was performed using GraphPad software version 5.01 for Windows (GraphPad Software). A *p* value <0.05 was considered statistically significant.

Results

Dimerization of Hp91 enhances DC uptake and activation

Since Cysteine residues, with an unprotected sulhydryl group, can form disulphide bridges, especially in oxidative conditions, we examined to what extent tertiary structure might affect Hp91 binding and activation of DCs. Hp91 was dissolved in PBS, incubated at room temperature for up to 96 h, and the presence of dimers was determined using HPLC. Hp91 dimers, which elute slower from the HPLC C18 column, constituted approximately 25% of the total peptide within 24 h. Dimers continued to form until measurements were stopped at 96 h, at which point greater than 80% of the Hp91 peptide was in a dimer formation (Figure 1A and B) and exposure of Hp91 to DTT caused 100% of the peptide maintain a monomer state (Figure 1C).

Since Hp91 dimerization occurs quickly in ambient oxygen conditions and could theoretically affect Hp91's interaction with DCs, we generated chemically stable capped Hp91 monomers and cross-linked Hp91 dimers using maleimide conjugation reactions. Mono- or bis-maleimides contain an imide group that reacts readily with the thiol group of cysteine to form a stable carbon-sulfur bond. NEM is a mono-maleimide that generates a capped peptide monomer. BM(Peg)₂ is a bis-maleimide that cross-links two peptides to form a dimer. In a representative experiment, HPLC of the untreated control Hp91 showed that an estimated 36% of peptide was in the dimer form (Figure 2A). HPLC of the maleimide conjugation products showed that the NEM capped monomer produced a single peptide peak, suggestive of close to 100% Hp91 peptide monomers, where the BM(PEG)₂ cross-linked dimer forms two peaks with an estimated 65% Hp91 peptide dimers (Figure

2B, C). We assessed the biological activity of these Hp91 monomers and dimers compared to control, as measured by activation of DCs and their ability to be taken up within DCs.

Like HMGB1, Hp91 is internalized by DCs (Supplemental Figure 1, manuscript in preparation), and can be assessed and quantified by flow cytometry on permeabilized cells (11). Confocal microscopy (Supplemental Figure 1) shows that Hp91 does not simply bind to the cell surface but quickly gets internalized into the cells. Uptake has been confirmed by timelapse confocal microscopy with fluorescently-labeled Hp91 (data not shown). Using the maleimide reaction products, we evaluated how tertiary structure affects the internalization of Hp91 peptide by DCs. The Hp91 monomer was incubated with DCs at 37° C for 30 min, and DC uptake was evaluated by flow cytometry. NEM-capped Hp91 monomer peptide showed 27% decreased uptake compared to control Hp91 peptide (Figure 2D). In contrast, dimerizing the Hp91 peptide with a bismaleimide reaction significantly increased cellular uptake by 3-fold (Figure 2E).

To evaluate whether the internalization of Hp91 peptide was associated with DC activation, DCs were stimulated with control Hp91 peptide or the maleimide reaction products and supernatants were analyzed after 48 hours for cytokine production. In concordance with the decreased uptake, the NEM-capped Hp91 monomer exerted a reduced immunostimulatory effect on the DCs with a 9-fold reduction in IL-6 secretion (Figure 2F). In contrast, dimerization of Hp91 enhanced the Hp91 immunostimulatory effect exerted on DC, with approximately 10-fold increased IL-6 secretion from Hp91 dimer-stimulated DCs compared to controls (Figure 2G). Together, these data show that dimerization of Hp91 peptide enhances DC activity and uptake.

Activity of Hp91 resides in C-terminal amino acids

In an effort to identify the region of Hp91 required for DC uptake and activation, overlapping 8–9 aa long peptides that span the length of Hp91 were synthesized and evaluated (Figure 3A). These short peptides were named UC (University of California) followed by the starting and ending aa residues in the Hp91 peptide sequence, e.g. amino acids 10–18 of Hp91 are called UC1018. To assess their activity, DCs were exposed to these short, overlapping peptides for 48 hours and supernatants were analyzed for IL-6. Compared to the media control, peptides UC714 and UC1018 significantly enhanced secretion of IL-6 by 12-fold and 27-fold respectively, while peptides UC18 and UC411 failed to induce cytokine secretion (Figure 3B). Peptides UC714 and UC1018 are within the C-terminal half of Hp91, indicating that the C-terminal portion is important for DC activation. When comparing to full-length Hp91 peptide, UC714 and UC1018 induced a significant increase in IL-6 secretion, but to a lesser extent compared to Hp91 (Figure 3B). This suggests that the C-terminal portion is necessary for IL-6 secretion, but not sufficient to induce full level of cytokine secretion *in vitro*.

Since Hp91 is internalized by DCs (Supplemental Fig. 1), we evaluated cellular binding of the short Hp91-derived peptides. DCs were incubated with equimolar doses of biotinylated versions of the short peptides for 30 minutes at 37°C to allow uptake. Cells were fixed, permeabilized, stained with streptavidin-Alexa 488, and evaluated by flow cytometry. The 9 aa acid long peptide UC1018, which corresponds to the C-terminal amino acids of Hp91,

resulted in a 3-fold enhanced binding to DCs as compared to Hp91. (Figure 3C and D). In contrast, UC18, UC411, and UC714, containing varying portions of the N-terminal 14 aa of Hp91, did not bind to DCs (Figure 3C). Additionally, maleimide reactions with UC1018 peptide demonstrated that the UC1018 peptide monomer fails to induce IL-6 secretion, whereas both control and maleimide-dimerized UC1018 were able to do so (Supplemental data, Figure 2). This suggests UC1018 acts on dendritic cells in a dimer state.

The C-terminal portion of Hp91 contains an α -helix

Since the C-terminal domain of Hp91, UC1018, is important for uptake and DC activation, we evaluated the secondary structure of this peptide using circular dichroism (CD). Based on previous studies of the secondary structure of HMGB1, we anticipated that the secondary structure at the UC1018 position within HMGB1 would contain an alpha helix (Figure 4A) (14). CD is sensitive to the secondary structure of polypeptides and can be used between wavelengths of 190–250 nm to analyze a peptide for different structural types such as alpha helix, beta sheet, polyproline II helix, or random coil. The CD spectrum of the C-terminal domain UC1018 demonstrated negative ellipticity bands at 207 and 222 nm, with a positive ellipticity at 198 nm (Figure 4B). Such a spectrum is characteristic of an alpha helix, matching our prediction for this amino acid sequence. The CD spectrum for the N-terminal peptide domain UC18 showed a negative maximum at 202 nm (Figure 4), which is close to the negative peak expected at 200 nm for a polyproline II helix. A spectrum with a negative peak around 200 nm is relatively ambiguous, as random coils also display similar spectra. However, since the N-terminal domain contains two PXXP motifs, which are known to form secondary structures of polyproline II helices (20), it is likely that the N-terminal domain UC18 is a polyproline II helix, rather than random coil. The CD spectrum for the entire length of Hp91 remains more difficult to interpret. The negative peak near 205 for Hp91 (Figure 4) may be an additive effect of the N-terminal- and C-terminal domain spectra negative maximums.

The short peptide UC1018 induces protective immune responses *in vivo*

Since the C-terminal half of Hp91 peptide was responsible for this peptide's *in vitro* activity, we set out to verify if it was similarly responsible for the *in vivo* activity of Hp91. We have previously shown (3) that full-length Hp91 peptide acts as adjuvant *in vivo* to induce antigen-specific immune responses. To evaluate if UC1018 would act as adjuvant to induce antigen-specific immune responses *in vivo*, mice were immunized with OVA-I (SIINFEKL) peptide as antigen and equimolar amounts of UC714, UC1018, or Hp91. In contrast to the UC714 peptide, immunization with UC1018 as adjuvant induced a significant increase in the number of antigen-specific IFN γ -secreting T cells compared to PBS controls which was 4-fold stronger than Hp91 (Figure 5A). Furthermore, IL-2, which is critical for the activation, survival, and proliferation of T lymphocytes, was significantly enhanced in mice immunized with UC1018, at levels 4-fold higher than Hp91 controls (Figure 5B). Since UC1018 induced a significantly enhanced antigen-specific immune response *in vivo*, we tested whether UC1018 induced immune responses were robust enough to protect mice from tumors. Mice were coimmunized with apoptotic B16 melanoma cells and either PBS or UC1018 peptide as adjuvant, and subsequently challenged with live B16 melanoma cells injected subcutaneously into the flank. The melanoma model used in this study is highly

lethal, such that within 7–10 days, the PBS control mice demonstrated tumor formation and rapid tumor growth, with the first mouse being sacrificed by day 16 post-challenge due to a substantial tumor burden (Figure 5C). In marked contrast to the PBS group, the UC1018 peptide immunized mice demonstrated a delay in tumor formation (Figure 5C), indicating an induction of significant protective antitumor immunity in the immunized mice where UC1018 had been used as adjuvant. The mice were monitored for survival, and mice that received the UC1018 prophylactic vaccine demonstrated a striking and significant enhancement of survival, with 60% of mice tumor-free and alive at 75 days post-tumor challenge (Figure 5D). In contrast, all mice in the control group developed tumor with 100% of mice succumbing to tumor burden by 49 days post-challenge (Figure 5D)

Discussion

There is a need for safer and more potent adjuvants (21, 22). We have previously shown that the 18 amino acid long peptide Hp91 acts as a potent stimulus for human DCs with the ability to generate a Th1-type immune response *in vitro* (10) and acts as adjuvant *in vivo*; inducing cellular immune responses to peptide and both cellular and humoral immune responses (3). The results presented here characterize the structural basis for Hp91 activity, demonstrating that Hp91 dimerization enhances activity and that the shorter 9 aa C-terminal fragment UC1018 acts as potent adjuvant *in vivo*.

We investigated what amino acid domains were responsible for the activity of the Hp91 immunostimulatory peptide. We show that Hp91 can form spontaneous dimers at ambient oxygen and dimerization significantly enhanced peptide uptake. Hp91 dimer also showed a consistent increase in DC activation, but the increase was not statistically significant, which is likely due to number of experiments run (n=3).

While the receptor(s) for Hp91 remain unknown, knowing that Hp91 peptide dimerization has enhanced activity may help us predict how Hp91 interacts with cells and generate hypotheses about potential receptors. It has long been known that toll-like receptors, such as TLR4, form homo- or hetero-dimers with other members of their protein family (23). Such TLR4 homodimers are thought to be necessary for recruitment of adaptor proteins and subsequent signaling. For example, the Mal and TRAM adaptor proteins are predicted to bind at the TLR4 homodimer interface (24). It is possible that dimerization of Hp91 peptide promotes receptor cross-linking, adaptor recruitment, and downstream signaling. By reconsidering the known molecular interaction of the parent protein, HMGB1, it may be possible to predict receptors for Hp91. Several receptors are implicated in HMGB1 mediated activation of cells, including the receptor for advanced glycation end-products (RAGE) (25, 26) toll-like receptor 2 (TLR2), TLR4 (11, 27–30), TLR9 (31), Mac-1 (32), syndecan-1 (33, 34), receptor-type tyrosine phosphatase- ζ/β (33, 35), and CD24/Siglec-10 (36). Preliminary experiments suggest that amino acids within the C-terminal half of Hp91 may be activating DCs through TLR4 (Supplemental Figure 3). Future work will investigate which receptors are involved in Hp91 DC interaction and signaling pathways,

We determined the region of the peptide responsible for biological activity by testing shorter, overlapping peptides for their potential to stimulate cytokine secretion from DCs,

and for their uptake by cells. Hp91 contains two PXXP motifs at the N-terminal half of the peptide, present in short peptides UC18 and UC411. PXXP motifs have been shown to bind to SH3 domains (20), thus we originally hypothesized that the activity of Hp91 may lie within the N-terminal portion. However, it was the C-terminal end, not the N-terminal end of the peptide that contained the biological activity, i.e. ability to activate DCs and function as adjuvant. We demonstrated that UC1018, despite being only half the length of Hp91, was taken up by DCs to a greater extent and was a 3-fold stronger adjuvant *in vivo*, as measured by IFN- γ and IL-2 responses. UC1018 is a potent adjuvant, conferring a strong protective anti-tumor immune response. In a prophylactic tumor vaccine using UC1018 as adjuvant, 60% of mice survived and were tumor free after 75 days in an aggressive melanoma model. Future studies will evaluate UC1018 for therapeutic tumor vaccines. It still remains to be determined how dimerization affects UC1018 peptide as adjuvant, and covalently coupled antigen-UC1018 peptide would be another vaccine approach. Another possibility to improve upon its potency would be the addition of non-HMGB1-derived antigenic amino acids (37) in an attempt to further increase adjuvanticity potential.

From a molecular point of view, UC1018 is a unique peptide, with an extremely hydrophobic N-terminal half, and a C-terminal CSE motif. Hydrophobicity has been shown to enhance cell penetrating properties of peptides (38) and based on this, one might predict that it is this hydrophobic region of UC1018, rich in phenylalanine, that is responsible for internalization by DCs. However, as this hydrophobic patch is also present in the UC714 peptide, which has no ability to be taken up by DCs, we reason that it is the CSE motif that is the critical sequence for DC binding and uptake. Interestingly, the cysteine residue in this CSE motif is the same cysteine that has previously been hypothesized to be critical for HMGB1's interaction with TLR4 (11).

The structure-function relationships demonstrated in this work may help the design of new synthetic adjuvant peptides. It is known that hydrophobic peptides act as danger signals to the immune system (39). Perhaps introducing hydrophobic regions, such as those found in the C-terminal half of Hp91, into synthetically designed adjuvants may enhance their activity, especially with regard to cytokine secretion.

We show here that the secondary structure of UC1018 peptide is an alpha helix. Perhaps this alpha helix plays a role in the adjuvanticity potential of peptides and could be designed into new synthetic vaccines containing adjuvant antigen fusions. The N-terminal half of Hp91 appeared to have no activity by itself, however we only performed uptake studies and examined cytokine secretion by DCs. This region, which contains two PXXP motifs, may have as yet unidentified activities that are important for HMGB1 or Hp91 activity. The region may be important for enhancing cytokine production, as the C-terminal domains stimulated DCs to secrete significantly less IL-6 than the full 18 aa Hp91. Additionally, this region may be responsible for intracellular activities that occur after Hp91 has entered a cell. For example, the polyproline II helix conformation of PXXP motifs, such as those in the C-terminal domain, is necessary for binding to intracellular Src homology-3 (SH3) domains (20).

In summary, we have investigated the activity of Hp91 immunostimulatory peptide, whose structure-function relationships had not been clear before now. We show that Hp91 dimerization enhances activity and that the helical C-terminus, UC1018, has DC binding and adjuvant activity that is stronger than full-length Hp91. We show promising tumor challenge results in which 60% of UC1018-immunized mice remained tumor-free after a highly lethal B16 challenge. This short peptide UC1018 warrants further investigation in immunization and mechanism studies. Additionally, deciphering the structure-function relationships of Hp91 and UC1018 may represent an important first step in the design of novel synthetic vaccine adjuvants.

Supplementary Material

Refer to Web version on PubMed Central for supplementary material.

Acknowledgments

We would like to thank I. Bharati and J.F. Fecteau for excellent technical assistance, and S. Sundelius and S. Sundqvist for their help with microscopy. Additionally, we would like to thank Paul Steinbach and the Roger Tsien lab for their assistance with live confocal imaging.

References

1. Steinman RM, Banchereau J. Taking dendritic cells into medicine. *Nature*. 2007; 449(7161):419–26. [PubMed: 17898760]
2. Dubensky TW Jr, Reed SG. Adjuvants for cancer vaccines. *Semin Immunol*. 2010
3. Saenz R, da Souza CS, Huang CT, Larsson M, Esener S, Messmer D. HMGB1-derived peptide acts as adjuvant inducing immune responses to peptide and protein antigen. *Vaccine*. 2010; 28(47): 7556–62. [PubMed: 20800114]
4. Agresti A, Bianchi ME. HMGB proteins and gene expression. *Curr Opin Genet Dev*. 2003; 13(2): 170–8. [PubMed: 12672494]
5. Rovere-Querini P, Capobianco A, Scaffidi P, Valentini B, Catalanotti F, Giazson M, et al. HMGB1 is an endogenous immune adjuvant released by necrotic cells. *EMBO Rep*. 2004; 5(8):825–30. [PubMed: 15272298]
6. Scaffidi P, Misteli T, Bianchi ME. Release of chromatin protein HMGB1 by necrotic cells triggers inflammation. *Nature*. 2002; 418(6894):191–5. [PubMed: 12110890]
7. Ulloa L, Messmer D. High-mobility group box 1 (HMGB1) protein: friend and foe. *Cytokine Growth Factor Rev*. 2006; 17(3):189–201. [PubMed: 16513409]
8. Wang H, Vishnubhakat JM, Bloom O, Zhang M, Ombrellino M, Sama A, et al. Proinflammatory cytokines (tumor necrosis factor and interleukin 1) stimulate release of high mobility group protein-1 by pituicytes. *Surgery*. 1999; 126(2):389–92. [PubMed: 10455911]
9. Messmer D, Yang H, Telusma G, Knoll F, Li J, Messmer B, et al. High mobility group box protein 1: an endogenous signal for dendritic cell maturation and Th1 polarization. *J Immunol*. 2004; 173(1):307–13. [PubMed: 15210788]
10. Telusma G, Datta S, Mihajlov I, Ma W, Li J, Yang H, et al. Dendritic cell activating peptides induce distinct cytokine profiles. *Int Immunol*. 2006; 18(11):1563–73. [PubMed: 16966494]
11. Yang H, Hreggvidsdottir HS, Palmblad K, Wang H, Ochani M, Li J, et al. A critical cysteine is required for HMGB1 binding to Toll-like receptor 4 and activation of macrophage cytokine release. *Proc Natl Acad Sci U S A*. 2010; 107(26):11942–7. [PubMed: 20547845]
12. Hoppe G, Talcott KE, Bhattacharya SK, Crabb JW, Sears JE. Molecular basis for the redox control of nuclear transport of the structural chromatin protein Hmgb1. *Exp Cell Res*. 2006; 312(18): 3526–38. [PubMed: 16962095]

13. Yang H, Lundback P, Ottosson L, Erlandsson-Harris H, Venereau E, Bianchi ME, et al. Redox modification of cysteine residues regulates the cytokine activity of high mobility group box-1 (HMGB1). *Mol Med*. 2012; 18:250–9. [PubMed: 22105604]
14. Thomas JO, Travers AA. HMG1 and 2, and related 'architectural' DNA-binding proteins. *Trends Biochem Sci*. 2001; 26(3):167–74. [PubMed: 11246022]
15. Bienkiewicz EA, Moon Woody A, Woody RW. Conformation of the RNA polymerase II C-terminal domain: circular dichroism of long and short fragments. *J Mol Biol*. 2000; 297(1):119–33. [PubMed: 10704311]
16. van Holst GJ, Fincher GB. Polyproline II Confirmation in the Protein Component of Arabinogalactan-Protein from *Lolium multiflorum*. *Plant Physiol*. 1984; 75(4):1163–4. [PubMed: 16663751]
17. Li SC, Goto NK, Williams KA, Deber CM. Alpha-helical, but not beta-sheet, propensity of proline is determined by peptide environment. *Proc Natl Acad Sci U S A*. 1996; 93(13):6676–81. [PubMed: 8692877]
18. Sonnichsen FD, Van Eyk JE, Hodges RS, Sykes BD. Effect of trifluoroethanol on protein secondary structure: an NMR and CD study using a synthetic actin peptide. *Biochemistry*. 1992; 31(37):8790–8. [PubMed: 1390666]
19. Jenne L, Arrighi JF, Jonuleit H, Saurat JH, Hauser C. Dendritic cells containing apoptotic melanoma cells prime human CD8+ T cells for efficient tumor cell lysis. *Cancer Res*. 2000; 60(16):4446–52. [PubMed: 10969791]
20. Yu H, Chen JK, Feng S, Dalgarno DC, Brauer AW, Schreiber SL. Structural basis for the binding of proline-rich peptides to SH3 domains. *Cell*. 1994; 76(5):933–45. [PubMed: 7510218]
21. Singh M, O'Hagan D. Advances in vaccine adjuvants. *Nature Biotechnology*. 1999; 17(11):1075–81.
22. McCluskie MJ, Weeratna RD. Novel adjuvant systems. 2001; 1(3):263–71.
23. Jin MS, Lee JO. Structures of the toll-like receptor family and its ligand complexes. *Immunity*. 2008; 29(2):182–91. [PubMed: 18701082]
24. Nunez Miguel R, Wong J, Westoll JF, Brooks HJ, O'Neill LA, Gay NJ, et al. A dimer of the Toll-like receptor 4 cytoplasmic domain provides a specific scaffold for the recruitment of signalling adaptor proteins. *PLoS One*. 2007; 2(8):e788. [PubMed: 17726518]
25. Hori O, Brett J, Slattery T, Cao R, Zhang J, Chen JX, et al. The receptor for advanced glycation end products (RAGE) is a cellular binding site for amphotericin. Mediation of neurite outgrowth and co-expression of rage and amphotericin in the developing nervous system. *The Journal of Biological Chemistry*. 1995; 270(43):25752–61. [PubMed: 7592757]
26. Dumitriu IE, Baruah P, Bianchi ME, Manfredi AA, Rovere-Querini P. Requirement of HMGB1 and RAGE for the maturation of human plasmacytoid dendritic cells. *Eur J Immunol*. 2005; 35(7):2184–90. [PubMed: 15915542]
27. Park JS, Gamboni-Robertson F, He Q, Svetkauskaite D, Kim JY, Strassheim D, et al. High mobility group box 1 protein interacts with multiple Toll-like receptors. *Am J Physiol Cell Physiol*. 2006; 290(3):C917–24. [PubMed: 16267105]
28. Park JS, Svetkauskaite D, He Q, Kim JY, Strassheim D, Ishizaka A, et al. Involvement of toll-like receptors 2 and 4 in cellular activation by high mobility group box 1 protein. *The Journal of Biological Chemistry*. 2004; 279(9):7370–7. [PubMed: 14660645]
29. van Zoelen MA, Yang H, Florquin S, Meijers JC, Akira S, Arnold B, et al. Role of Toll-Like Receptors 2 and 4, and the Receptor for Advanced Glycation End Products (Rage) in Hmgb1 Induced Inflammation in Vivo. *Shock*. 2008
30. Yu M, Wang H, Ding A, Golenbock DT, Latz E, Czura CJ, et al. HMGB1 signals through toll-like receptor (TLR) 4 and TLR2. *Shock*. 2006; 26(2):174–9. [PubMed: 16878026]
31. Ivanov S, Dragoi AM, Wang X, Dallacosta C, Louten J, Musco G, et al. A novel role for HMGB1 in TLR9-mediated inflammatory responses to CpG-DNA. *Blood*. 2007; 110(6):1970–81. [PubMed: 17548579]
32. Orlova VV, Choi EY, Xie C, Chavakis E, Bierhaus A, Ihanus E, et al. A novel pathway of HMGB1-mediated inflammatory cell recruitment that requires Mac-1-integrin. *EMBO J*. 2007; 26(4):1129–39. [PubMed: 17268551]

33. Rauvala H, Rouhiainen A. Physiological and pathophysiological outcomes of the interactions of HMGB1 with cell surface receptors. *Biochim Biophys Acta*. 2010; 1799(1–2):164–70. [PubMed: 19914413]
34. Salmivirta M, Rauvala H, Elenius K, Jalkanen M. Neurite growth-promoting protein (amphoterin, p30) binds syndecan. *Exp Cell Res*. 1992; 200(2):444–51. [PubMed: 1369684]
35. Milev P, Chiba A, Haring M, Rauvala H, Schachner M, Ranscht B, et al. High affinity binding and overlapping localization of neurocan and phosphacan/protein-tyrosine phosphatase-zeta/beta with tenascin-R, amphoterin, and the heparin-binding growth-associated molecule. *J Biol Chem*. 1998; 273(12):6998–7005. [PubMed: 9507007]
36. Chen GY, Tang J, Zheng P, Liu Y. CD24 and Siglec-10 selectively repress tissue damage-induced immune responses. *Science*. 2009; 323(5922):1722–5. [PubMed: 19264983]
37. Patel A, Dong JC, Trost B, Richardson JS, Tohme S, Babiuk S, et al. Pentamers not found in the universal proteome can enhance antigen specific immune responses and adjuvant vaccines. *PLoS One*. 2012; 7(8):e43802. [PubMed: 22937099]
38. Pujals S, Giralt E. Proline-rich, amphipathic cell-penetrating peptides. *Adv Drug Deliv Rev*. 2008; 60(4–5):473–84. [PubMed: 18187229]
39. Seong SY, Matzinger P. Hydrophobicity: an ancient damage-associated molecular pattern that initiates innate immune responses. *Nat Rev Immunol*. 2004; 4(6):469–78. [PubMed: 15173835]

Highlights

The immunostimulatory activity of HMGB1 derived peptide Hp91 is enhanced by dimerization

The C-terminal 9 amino acids of HP91 are sufficient for dendritic cell activation

A peptide composed of the 9 c-terminal amino acids of HP91, named UC1018) induced potent CTL responses *in vivo*

When combined with a tumor antigen, UC1018 protected mice from subsequent tumor challenge

UC1018 adopts a helical structure

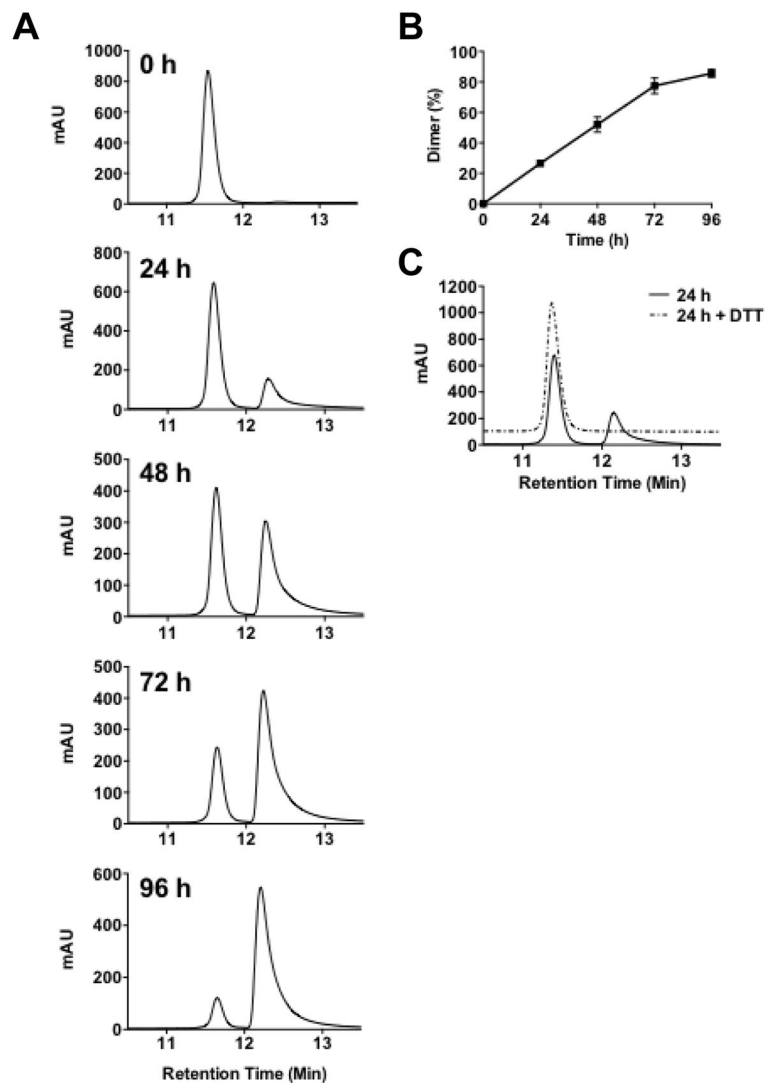


Figure 1. Hp91 forms spontaneous, reversible dimers

(A–B) Hp91 peptide was dissolved in PBS and incubated at RT in the presence of ambient oxygen for up to 96 h. Peptides were analyzed by HPLC. Peptide monomers show a peak at an earlier time point than the peptide dimers (12.2 min vs. 12.7 min respectively). Percent dimer was determined by measuring the area under the curve (AUC) and calculating the dimer AUC/total AUC. Results shown are (A) representative of several independent experiments and (B) mean (\pm SEM) for $n=3-4$. (C) Peptides incubated with Hp91 for 24 hours were subsequently incubated \pm 10 mM DTT for 30 minutes prior to analysis by HPLC. DTT incubated sample offset on graph for ease of viewing. Results are representative of two independent experiments.

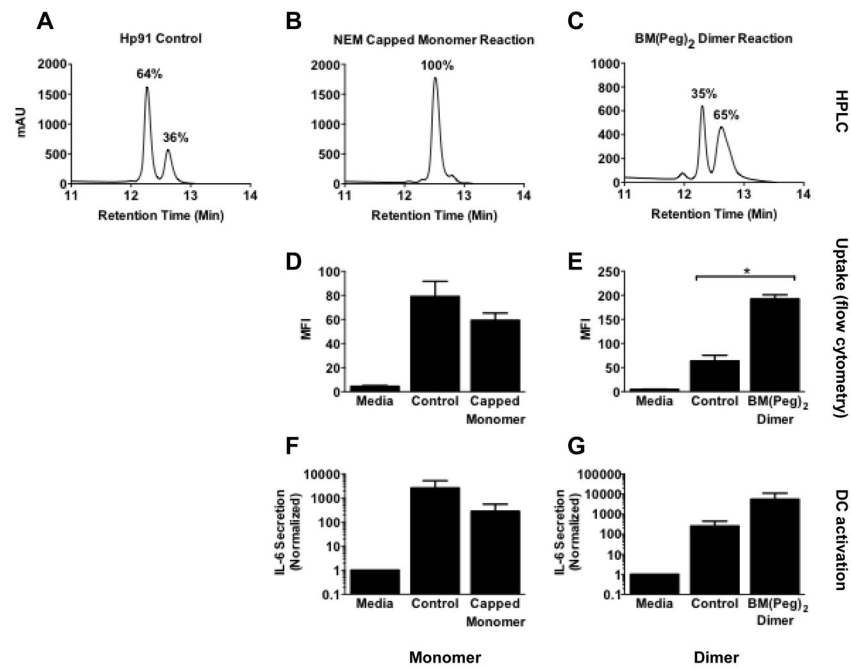


Figure 2. Dimerization of Hp91 enhances DC binding and activation

(A–C) Hp91 peptide control, NEM capped monomer reaction product, or BM(PEG)₂ cross-linked dimer were analyzed by HPLC. Percent dimer was determined by measuring the AUC and calculating the dimer AUC/total AUC. (D) Immature human DCs were pre-cooled on ice for 30 minutes, then incubated with media only or 100µg/ml of biotinylated-Hp91 (Control) or the biotinylated Hp91 NEM monomer reaction product (Capped Monomer) for 60 minutes at 37°C. Cells were permeabilized with Cytofix/Cytoperm, stained with streptavidin-Alexa 488, and analyzed by flow cytometry. Results shown are mean (±SEM) for 3 independent experiments. $p > 0.05$. (E) Immature human DCs were pre-cooled as above and incubated with media only or 56µg/ml of biotinylated-Hp91 (Control) or biotinylated Hp91 BM(PEG)₂ cross-linked reaction product (BM(PEG)₂ Dimer) for 60 minutes at 37°C. Cells were permeabilized and stained as above and analyzed by flow cytometry. Results shown are mean (±SEM) for $n=3$. * $p < 0.05$; Student's t-test. (F) Immature DCs were incubated with media only or 100µg/ml un-reacted acetylated Hp91 (Control), or an acetylated Hp91 NEM monomer reaction product (Capped Monomer). Supernatants were collected after 48 h and analyzed for the presence of IL-6 by ELISA. Data are normalized with respect to media controls. Results are mean (±SEM) for $N=3$. (G) Immature DCs were incubated with media only or 56µg/ml un-reacted acetylated Hp91 (Control), or an acetylated Hp91 BM(PEG)₂ cross-linked reaction product (BM(PEG)₂ Dimer). Supernatants were collected after 48 h and analyzed for the presence of IL-6 by ELISA. Data are normalized with respect to media controls. Results are mean (±SEM) for $n=3$.

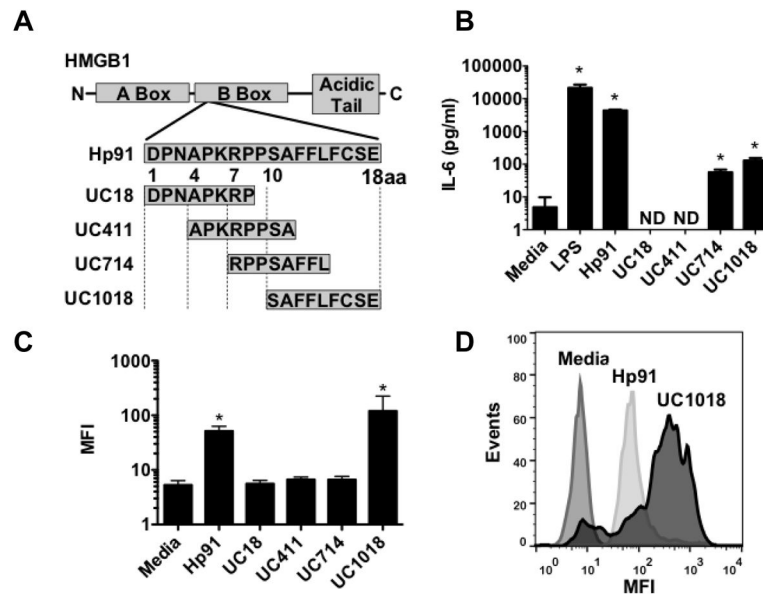


Figure 3. Immunostimulatory activity of Hp91 short peptides

(A) Four short (8–9 aa) overlapping peptides that span Hp91 were synthesized. (B) Immature DCs were stimulated with the indicated peptides at 90 μ M for 48 h. Supernatants were analyzed for the presence of IL-6 by ELISA. Data are mean (\pm SEM) for 3 independent experiments. None detected (ND) is noted where applicable. (C, D) Immature DCs were pre-cooled on ice for 30 minutes, then incubated with medium only or the indicated biotinylated peptides at 90 μ M for 30 minutes at 37 $^{\circ}$ C. Cells were then permeabilized, stained with streptavidin-Alexa 488, and uptake was analyzed by flow cytometry. (C) is mean (\pm SEM) of independent experiments (n=3) and (D) is a representative result. *p < 0.05 compared to media controls; Student's t-test or ANOVA, as applicable.

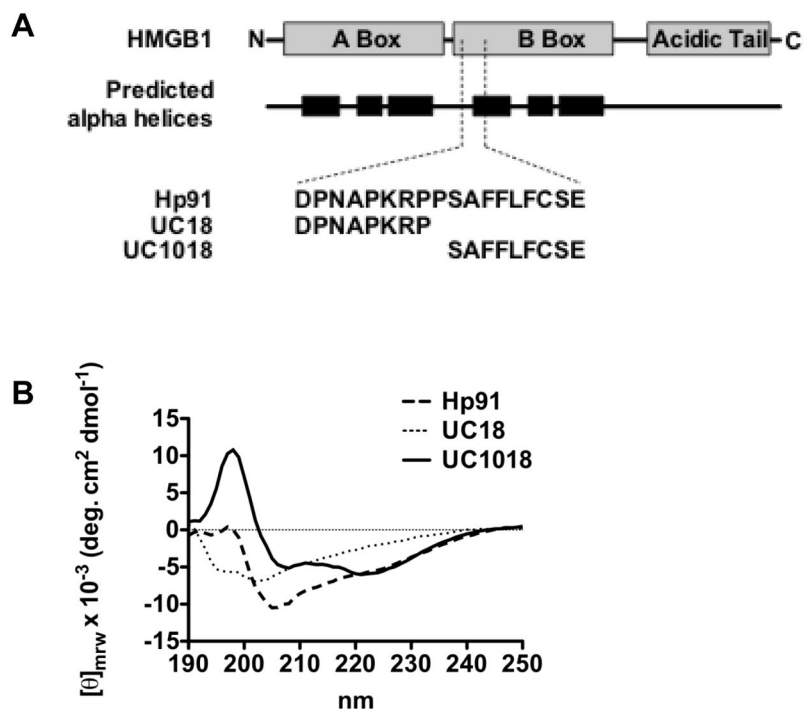


Figure 4. Circular dichroism suggests alpha helical shape of UC1018

(A) HMGB1 molecular architecture and locations of predicted alpha helices (14) compared to Hp91 and its peptide fragments. (B) Hp91, UC18, and UC1018 were dissolved in 75%/25% TFE/H₂O (vol/vol) at 200μg/ml and CD spectra were collected on an AVIV Circular Dichroism Spectrometer using a 1mm pathlength quartz cuvette. These spectra were corrected by subtraction of a “solvent-only” spectrum and smoothed. The spectra are shown in mean residue ellipticity (θ_{mrw}). The Hp91 curve is representative of two independent experiments.

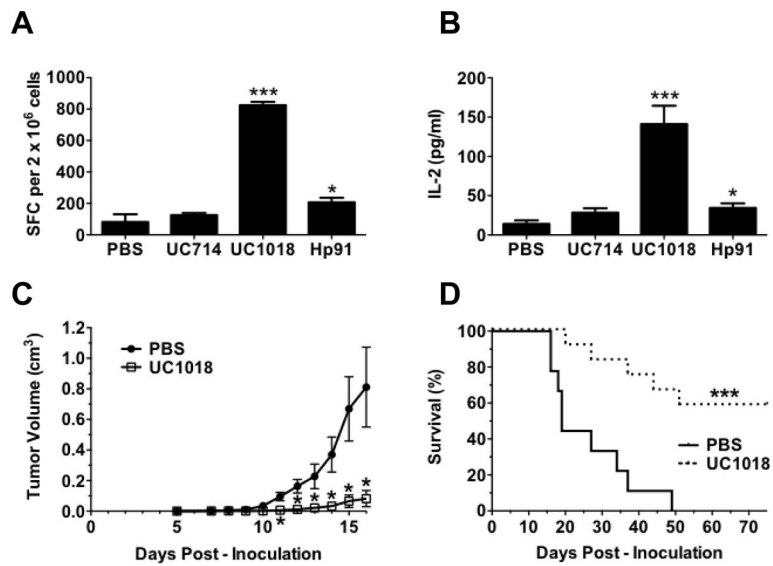


Figure 5. The short alpha helical peptide UC1018 induces protective immune responses in vivo (A, B) Mice were co-immunized with OVA-I (SIINFEKL) peptide with PBS (negative) or equimolar doses of Hp91 (250 μ g), UC714 (129 μ g), or UC1018 (142 μ g). Freshly isolated splenocytes from the immunized mice were cultured in the presence of SIINFEKL peptide (2.5 μ g/ml) in an (A) IFN- γ ELISpot assay, wherein the number of IFN- γ -secreting cells, or spot-forming cells (SFC), was determined 18 h later, or (B) culture supernatants were collected and analyzed for IL-2 secretion by ELISA. The data are shown as mean (\pm SEM) for at least 5 mice/group. * $p < 0.05$, or *** $p < 0.001$ compared to PBS; Student's t-test. (C, D) Mice were immunized s.c. with apoptotic mitomycin-C treated B16 cells co-injected with PBS (negative) or UC1018 peptide adjuvant (142 μ g) and boosted twice. One week post boost, mice were inoculated s.c. on the flank with 5×10^5 live B16 cells. (C) Tumor dimensions were measured over time. The data shown is mean (\pm SEM) for at least 14 mice/group. * $p < 0.01$ compared to PBS; Student's t-test at each time point. (D) Depicted is the percentage of surviving mice. Mice were euthanized when tumor volume reached 1.5 cm³. Tumor survival curves were generated, wherein the day of euthanasia was considered as death. *** $p < 0.001$ compared to PBS; Log rank test.